



**HAL**  
open science

## Single-frequency tunable VECSEL around the Cesium D2 line

Benjamin Cocquelin, Gaëlle Lucas-Leclin, Patrick Georges, Isabelle Sagnes,  
Arnaud Garnache

► **To cite this version:**

Benjamin Cocquelin, Gaëlle Lucas-Leclin, Patrick Georges, Isabelle Sagnes, Arnaud Garnache. Single-frequency tunable VECSEL around the Cesium D2 line. Photonics West - LASE 2008, Jan 2008, San Jose, United States. pp.687112.1-687112.9, 10.1117/12.763119 . hal-00531358

**HAL Id: hal-00531358**

**<https://hal-iogs.archives-ouvertes.fr/hal-00531358>**

Submitted on 2 Nov 2010

**HAL** is a multi-disciplinary open access archive for the deposit and dissemination of scientific research documents, whether they are published or not. The documents may come from teaching and research institutions in France or abroad, or from public or private research centers.

L'archive ouverte pluridisciplinaire **HAL**, est destinée au dépôt et à la diffusion de documents scientifiques de niveau recherche, publiés ou non, émanant des établissements d'enseignement et de recherche français ou étrangers, des laboratoires publics ou privés.

# Single-frequency tunable VECSEL around the Cesium D<sub>2</sub> line

B. Cocquelin<sup>1</sup>, G. Lucas-Leclin<sup>1</sup>, P. Georges<sup>1</sup>, I. Sagnes<sup>2</sup>, A. Garnache<sup>3</sup>

<sup>1</sup> Laboratoire Charles Fabry de l'Institut d'Optique, CNRS, Univ. Paris Sud, Campus Polytechnique, RD 128, 91127 Palaiseau, France

<sup>2</sup> Laboratoire de Photonique et de Nanostructures, Route de Nozay CNRS UPR 20, 91460, Marcoussis, France

<sup>3</sup> Institut d'Électronique du Sud, CNRS UMR5214, Université Montpellier 2, 34095 Montpellier, France

## ABSTRACT

This work reports on an optically-pumped vertical external-cavity surface-emitting laser (VECSEL) emitting around 852 nm for Cesium atomic clocks experiments. We describe the design and the characterization of a VECSEL semiconductor structure suitable for these applications. The parameters of the structure have been optimized in order to have a low threshold and a high gain structure emitting around 852 nm. We achieved an output power of 330 mW for 1.1 W of incident pump power. We are able to simulate the laser emission variations with the temperature of the substrate, the pump radius on the semiconductor structure and the losses inside cavity. A compact and robust setup was built to obtain a stable single-frequency emission. We obtained a 17-mW single frequency emission exhibiting broad and fine tunability around the Cesium D<sub>2</sub> line.

**Keywords:** Optically pumped semiconductor, VECSEL, Cesium atomic clocks, single-frequency emission

## 1. INTRODUCTION

Optically-pumped Vertical External-Cavity Surface-Emitting Lasers (VECSEL) combine the approach of diode-pumped solid-state lasers and engineered semiconductor lasers, generating both circular diffraction limited output beams and high average powers [1-3]. These lasers benefit from the knowledge in semiconductor fabrication and the power scaling possibilities of these thin disks to obtain high powers at the desired wavelength. Furthermore a homogeneous gain results from the resonant periodic gain design of the active structure. VECSELs appear then to be an interesting way to achieve compact and efficient single-frequency sources for demanding applications such as metrology and spectroscopy [4].

Our work is focused on the design of a laser structure suitable for Cesium atomic clock experiments. In these systems, the ideal laser source would merge a high power (>200 mW) for atom cooling, and a narrow linewidth (<500 kHz) for detection on an absorption line. Currently these specifications are achieved with multiple laser sources. According to [5] and [6], a single optically-pumped VECSEL should fulfil these two requirements in a compact set-up.

In this paper we present firstly the design of a specific structure emitting near 852 nm - corresponding to the Cs D<sub>2</sub> line - with a few quantum wells (QWs) in order to get a low threshold pump power and still a relatively high optical gain. Full optical and thermal characterizations of this structure have been carried out in order to investigate its intrinsic limitations. The third part of this work is the optimization of the laser output power. Finally we describe the results obtained with a compact and robust cavity at the Cesium D<sub>2</sub> line.

## 2. VECSEL STRUCTURE: DESIGN AND CHARACTERIZATION

### 2.1 Structure design and fabrication

The semiconductor structure is specifically designed for laser emission around 852 nm. It was grown by metal-organic chemical-vapor deposition on a 350- $\mu$ m thick GaAs substrate. It includes a multilayer Distributed Bragg Reflector (DBR) bottom mirror and an active region. The DBR bottom mirror consists of 29.5 pairs of AlAs/AlGaAs quarter-wave layers resulting in a 70-nm stop-band, reaching 99.95 % reflectivity at 852 nm (Figure 1). The active layer contains N (N = 4 or 7) 8-nm thick quantum wells (QWs) between AlGaAs barriers which are distributed among the optical standing-wave antinodes position in such a manner that the carrier density remains almost equal in all QWs. The active

layer thickness is  $9\lambda/2$  for the N=4 QWs structure, and  $29\lambda/4$  for the N = 7 QWs one. The pump wavelength must be below 730 nm for an efficient absorption in the AlGaAs barriers. Because of the low brightness of pump sources in this spectral range, the number of QWs in the gain region has been reduced to get a low threshold pump intensity but still a gain of about 1% to compensate for cavity losses (Figure 2). The top of the structure is protected from oxidation by GaAs and InGaP capping layers, and is anti-reflection (AR) coated at 852 nm with a  $\lambda/4$   $\text{Si}_3\text{N}_4$  layer to optimise the absorption of the incident pump laser and to reduce any intracavity etalon effect at the laser wavelength. The pump absorption is evaluated to 76% (N=4) and 88% (N=7) in the barriers. Since the optical pumping is off-axis ( $70^\circ$  with respect to the normal of the semiconductor surface) some residual reflection of the pump remains at the semiconductor/air interface resulting in a total absorption of the incident power of respectively 75% for N=4 and 86% for N=7.

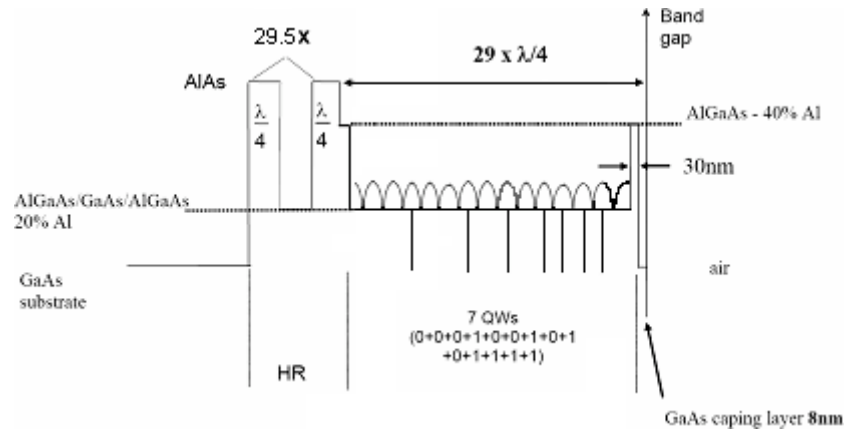


Fig. 1: Design of the semiconductor structure

Measurements of the reflectivity and the photoluminescence of the structures have been performed to check the epitaxial growth quality (Figure 2). The reflectivity spectrum exhibits a rectangular high reflectivity stop band centered on the desired lasing wavelength. It contains a dip representing absorption within the quantum wells enhanced by the micro cavity resonance. The photoluminescence spectrum of the quantum wells matches the micro cavity resonance suggesting the good laser properties of this structure.

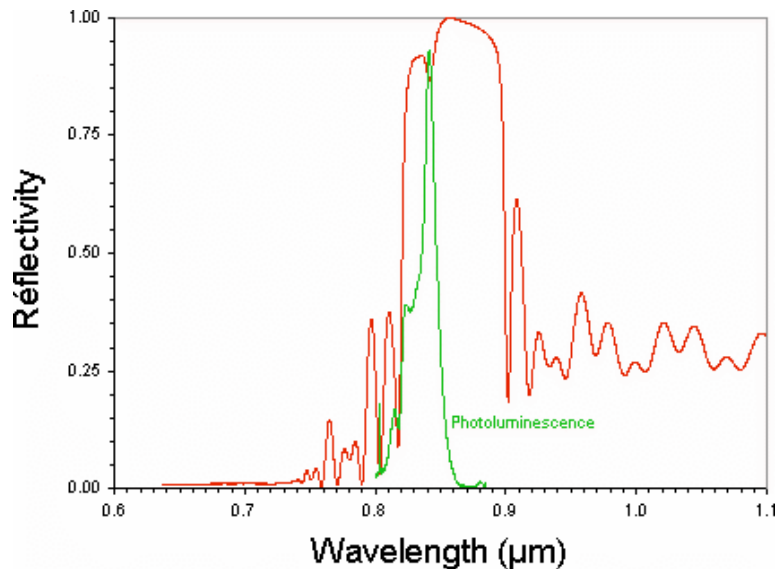


Fig. 2: Measured reflectivity and reflectivity of the semiconductor structure

## 2.2 Gain measurements

Gain measurements have been carried out in order to check whether the structure provides a high gain of few percents and low losses to have a low laser threshold and a good laser slope efficiency. For these experiments, the structure was optically pumped with a laser diode module emitting at  $\lambda_p = 690$  nm and coupled in a 100 $\mu$ m-core fibre. This source delivered a maximum output power of 5 W and was focused on a 40  $\mu$ m spot radius. The three-mirror cavity was composed of the DBR mirror, a 100-mm radius of curvature concave mirror with high reflectivity at  $\lambda_l = 852$  nm ( $R > 99.97\%$ ) and a plane output coupler (Figure 3). The semiconductor structure was fixed on a copper heatsink using heatpaste which temperature  $T_{sub}$  was controlled by a Peltier cooler.

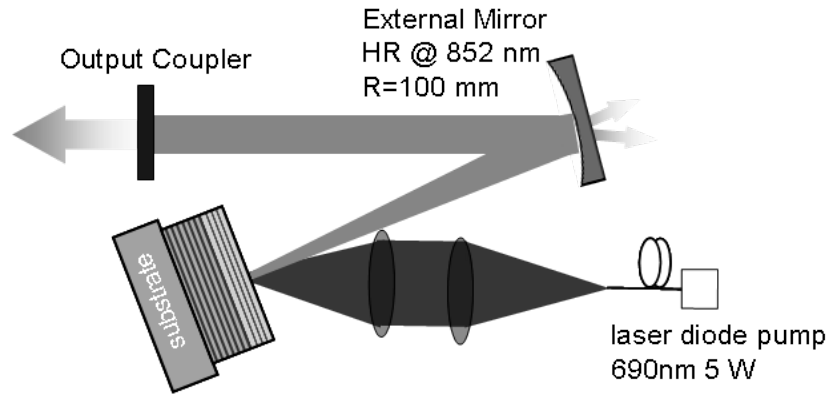


Fig. 3: Experimental setup

From the measurement of the laser threshold with various output couplers, a linear gain per well  $g_0 = 1000$   $\text{cm}^{-1}$  and an incident pump intensity at transparency per quantum well  $I_{tr} = 225$   $\text{W}/\text{cm}^2$  have been deduced (Figure 4). The optical losses inside the semiconductor structure have been evaluated to 0.3 % per round-trip. These experimental results have been compared with simulations based on the following equation [7]:

$$G(I_{inc}, N_{QW}) = 2L_{QW} N_{QW} \Gamma g_0 \ln \left( \frac{I_{inc}}{N_{QW} I_{tr}} \right) \quad (1)$$

where  $L_{QW}$  and  $N_{QW}$  represent respectively the thickness and the number of the QWs,  $\Gamma = 2$  is the longitudinal confinement factor and  $I_{inc}$  the incident pump intensity.

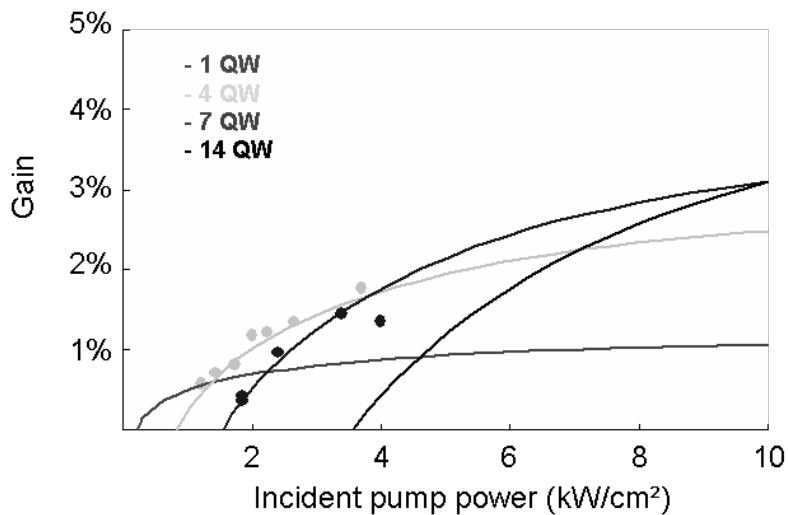


Fig. 4: Experimental gain measurement vs. pump intensity on the 4 QW and 7 QW structure and simulations for various numbers of QWs -  $T = 283$  K

We have plotted the gain of a structure with various number of quantum wells. From Figure 4 it is obvious that 7 QWs is the optimum choice for optical losses of few percents: less QWs would result in an insufficient gain, whereas more QWs would excessively increase the laser threshold. In the following we present the characterization and the performances of a 7 QW structure.

### 2.3 Thermal characterization

The output power of VECSEL is known to be limited by the heat load deposited in the active region by a fraction  $\eta_{th}$  of the incident pump power  $P_{inc}$ . The poor thermal conductivity of the semiconductor materials used in such devices prevents the thermal load dissipation, leading to a temperature increase with the pump power. Thus it is worth studying the thermal properties of the 7 QW structure.

The temperature raise is more important as the incident pump power, the thermal fraction  $\eta_{th}$  and the thermal resistance  $R_{th}$  are higher:

$$T_{QW} = T_{sub} + \eta_{th} R_{th} P_{inc} \quad (2)$$

The thermal fraction takes into account the quantum defect  $\lambda_p/\lambda_l$ , the internal quantum efficiency and the absorption in the DBR mirror. It is evaluated to 48 % for a 7 QW structure under the laser threshold and 31% above, since the internal quantum efficiency is around 70% under the threshold and rises to 95 % above.

Furthermore the thermal resistance of our 7 QWs component has been evaluated by measuring the evolution of the emitted wavelength firstly with respect to the incident pump power at a given temperature, secondly with respect to the temperature of the substrate at a given pump power :

$$R_{th} = \frac{\left(\frac{d\lambda}{dP_{th}}\right)_T}{\left(\frac{d\lambda}{dT}\right)_P} = \frac{\left(\frac{d\lambda}{dP_{inc}}\right)_T}{\left(\frac{d\lambda}{dT}\right)_P} \times \frac{1}{\eta_{th}} \quad (3)$$

For the first measurement the structure was optically pumped in a quasi-CW regime in order to prevent heating of the structure by the pump power. The pulses duration were 2.6  $\mu$ s and the repetition rate was 1 kHz. We measured a wavelength shift with the incident pump power of 15 nm/W at room temperature with a 0.2% output coupler. The second experiment demonstrated a wavelength shift with the temperature of 0.26 nm/K, close to the classical value of 0.3 nm/K for AlGaAs compounds. Using this method, we determined a thermal resistance of 184 K/W (with respect to the incident pump power) for a pump radius of 40  $\mu$ m. We deduce the theoretical value (187 K/W) from a simple three-layer analytical model under the same operating conditions [8]: we assumed a 1D heat flow in the thin active layers, leading to a contribution to the thermal resistance of the VECSEL active chip given by :

$$R_{th}^a = \frac{e}{\kappa_a \pi \omega_p^2} = 43K / W \quad (4)$$

with  $\kappa_a$  the thermal conductivity of the active layers (QWs + Bragg),  $e$  their total thickness and  $\omega_p$  the pump radius [8]; the 350  $\mu$ m-thick GaAs substrate contributes to :

$$R_{th}^s = \left(\kappa_s \pi \omega_p\right)^{-1} = 144K / W \quad (5)$$

following a 3D heat flow model more suitable for thick layers. The major contribution in the thermal resistance is due to the substrate. Thermal management techniques consist usually in reducing this contribution by removing the substrate [1-3] or bonding the active region on a higher conductivity substrate [9]. A heatspreader can also be placed inside the cavity to provide heat extraction from the top of the structure. [5,10]

## 3. OPTIMISATION OF THE OUTPUT POWER

From equations (2-5) we are able to determine the temperature in the active region under any substrate temperature, pump radius or incident pump power. We can now optimize the output power extracted from the semiconductor structure

based on the knowledge of its gain and thermal properties. Three main parameters can be optimized to achieve the highest output power from the semiconductor device. They are the temperature of the substrate and the pump radius (via the thermal resistance) which influence the heating of the semiconductor device, and the transmission of the output coupler which changes the cavity losses and the laser slope efficiency. We have studied the influence of each one of them on the laser properties, both experimentally and theoretically.

the temperature of the active region that determines the roll over apparition, and to the cavity losses related to the gain of the structure.

We have measured firstly the influence of the pump radius on the laser output power at room temperature. The 7-quantum-well semiconductor structure was placed in the three-mirror cavity (Figure 3) with an output coupler of 1.1%. The temperature of substrate is maintained at 293 K. We obtained a maximum laser output power of 125 mW under a pump power of 780 mW focused on a  $w_p = 40 \mu\text{m}$  radius (Figure 5). These results are in good agreement with simulations based on the following classical equation:

$$P_{\text{las}} = \eta_{\text{diff}} \left( P_{\text{inc}} - P_{\text{th}} \left[ T_{\text{QW}} \right] \right) \tag{6}$$

$$P_{\text{th}} \left[ T_{\text{QW}} \right] = P_0 \exp \left( \frac{T_{\text{QW}}}{T_0} \right) \tag{7}$$

Where  $P_{\text{las}}$  is the laser output power;  $\eta_{\text{diff}}$  is the differential efficiency (which is evaluated experimentally to 36 % in our operating condition);  $P_{\text{inc}}$  is the incident pump power.  $P_{\text{th}}$  is the laser threshold that critically depends on the temperature of the active region  $T_{\text{QW}}$ , following the exponential empirical law (Eq.7). To fit the experimental data, the characteristic temperature  $T_0$  is evaluated to 60 K. The temperature in the active region rises to 343 K at the maximum pump power. Above this critical point, the roll over occurs. Using equation (1) and (2), we can simulate the laser output power for different pump radii. Our simulation showed that  $40 \mu\text{m}$  is good optimum for our operational conditions.

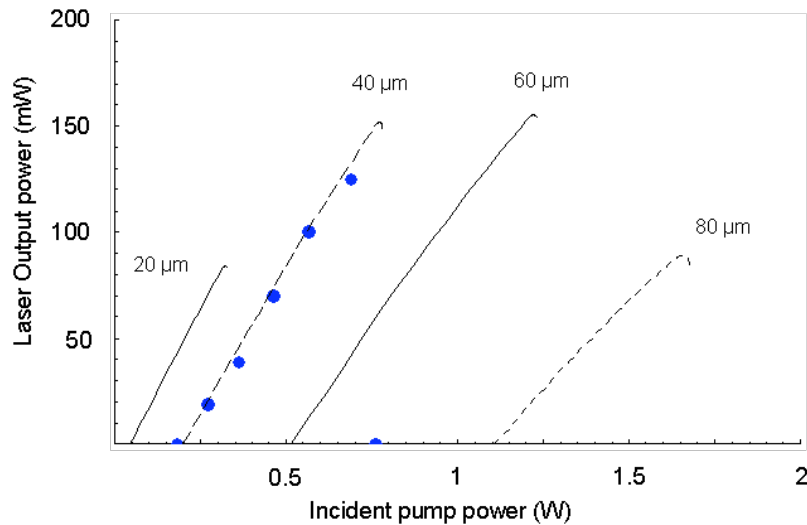


Fig. 5. Output power for different pump radii from  $20 \mu\text{m}$  to  $80 \mu\text{m}$  vs. the incident pump power on the semiconductor structure at room temperature (293 K): Experiment (dots) and simulations (solid and dashed lines)

The pump beam is from now focalized on the semiconductor structure on a  $40\mu\text{m}$  radius. We then changed the transmission of the plane output coupler in our three mirror cavity. The laser threshold and the slope efficiency of the laser increase with the transmission of the output coupler and reach a maximum for a 1 % transmission output coupler. This coupler is used in the following.

Transmission of the output coupler	Slope efficiency	Laser threshold $P_{th}$	Maximum output power
0.1%	6 %	2.3 kW/cm <sup>2</sup>	33 mW
0.7 %	23 %	2.9 kW/cm <sup>2</sup>	125 mW
1.1 %	26 %	3.7 kW/cm <sup>2</sup>	125 mW

**Table 1: Laser parameters evolution with the transmission of the output power at room temperature  $T_{sub}= 293$  K**

Finally, the temperature of the substrate was changed from 273 K to 293 K (Figure 6). A 10 K-raise in the temperature of the substrate increased the laser threshold from 3 kW/cm<sup>2</sup> to 3.7 kW/cm<sup>2</sup>, while decreasing the slope efficiency from 31% to 25%. At 273 K, we achieved 330 mW for pump power of 1.1 W. The slope efficiency reached 36 %. These high output powers performed on a GaAs substrate device demonstrate the well-thought design of the active structure and the quality of the fabrication process. The further increase of the output power will require a reduction of the VECSEL thermal resistance in order to withstand high-power pumping without roll-over. Standard solutions such as removing the GaAs substrate and soldering the structure onto a high-conductivity substrate or a heatsink could be used.

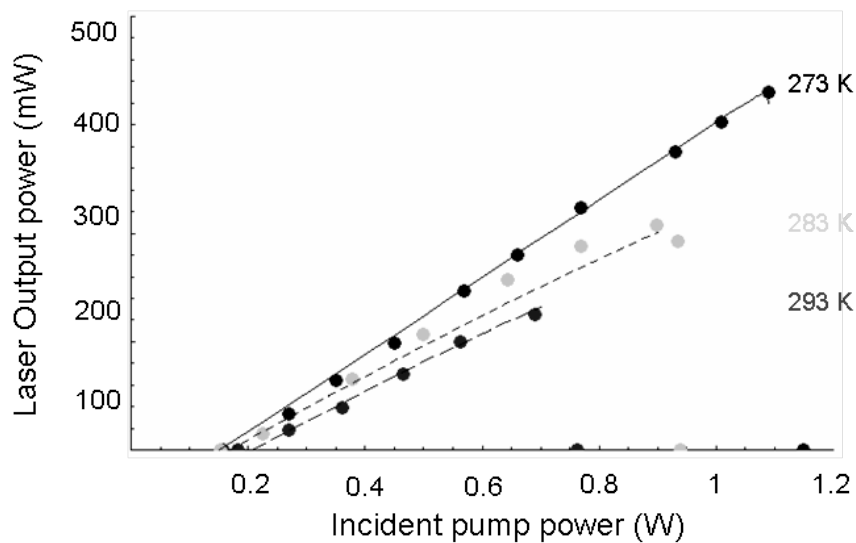


Fig. 6. Output power for different temperatures of the substrate  $T_{sub}= 273$  K, 283 K and  $T = 293$  K vs. the incident pump power on the semiconductor structure: Experiment (dots) and simulation (solid and dashed lines)

#### 4. SINGLE-FREQUENCY RESULTS

With the aim to develop a low-power single-frequency source dedicated to the detection of Cesium atoms, a short monolithic external cavity with improved mechanical stability has been designed. The pump source was a circular single transverse mode GaAlInP red laser diode delivering up to 150 mW at 658 nm for an operating current of 245 mA. The pump beam was focused on a 20  $\mu$ m radius spot with an incidence angle of 70°. The device was cooled at 280 K. The external cavity was formed by a 12 mm-concave mirror  $R = 99$  % at 852 nm mounted on a piezoelectric ceramic (Figure 7). The Free Spectral Range (FSR) of this compact cavity was 12.5 GHz.

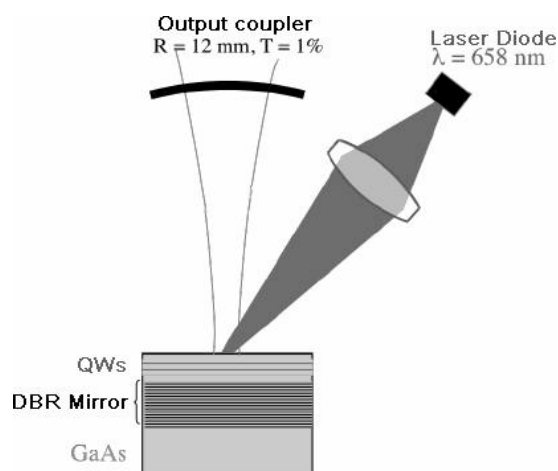


Fig. 7: Scheme of the VECSEL compact cavity

The maximum output power obtained was 17 mW under 150 mW pump power, only limited by the available pump power. The emission was linearly polarized with a good beam quality ( $M^2 < 1.2$ ). The threshold was reached for an incident pump intensity of  $4.1 \text{ kW/cm}^2$ . The slope efficiency was then 17% without any evidence of thermal roll-over. The emitted wavelength shifted from 850.5 nm at threshold to 852.2 nm at maximum pump power. The single-frequency operation was checked with a high finesse ( $F=130$ ) scanning Fabry Perot (Figure 8, inset) with a FSR of 37.5 GHz larger than the FSR of the laser cavity.

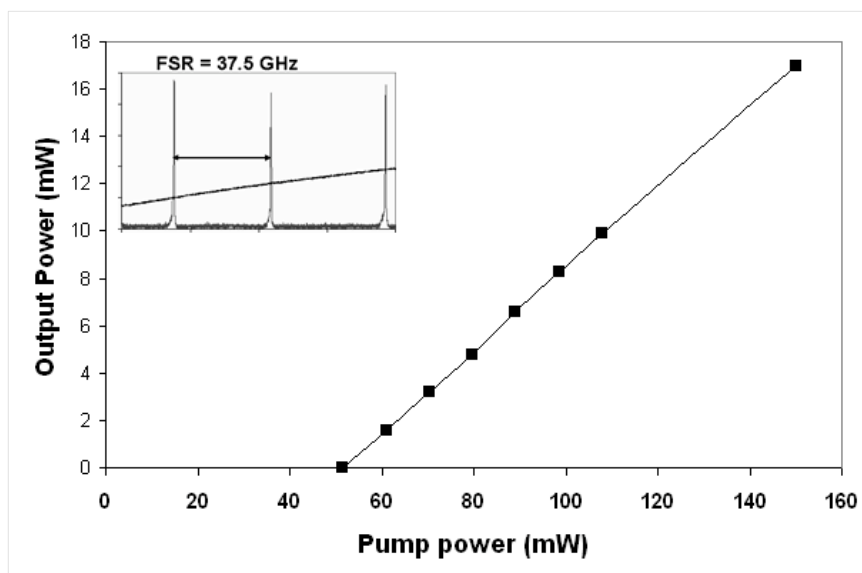


Fig. 8: Laser output power vs. incident pump power in a single frequency operation at 280 K; inset: Transmission of the scanning 37.5 GHz-FSR Fabry-Perot.

By tuning the external-cavity length with the piezoelectric ceramic, we achieved a continuous tunability over 14 GHz without any mode hop (Figure 9), which has been checked with a fixed 1.5 GHz-FSR Fabry-Perot. The laser wavelength at threshold was shifted over 6 nm from 850 nm to 856 nm by changing the substrate temperature from 280 K to 293 K.

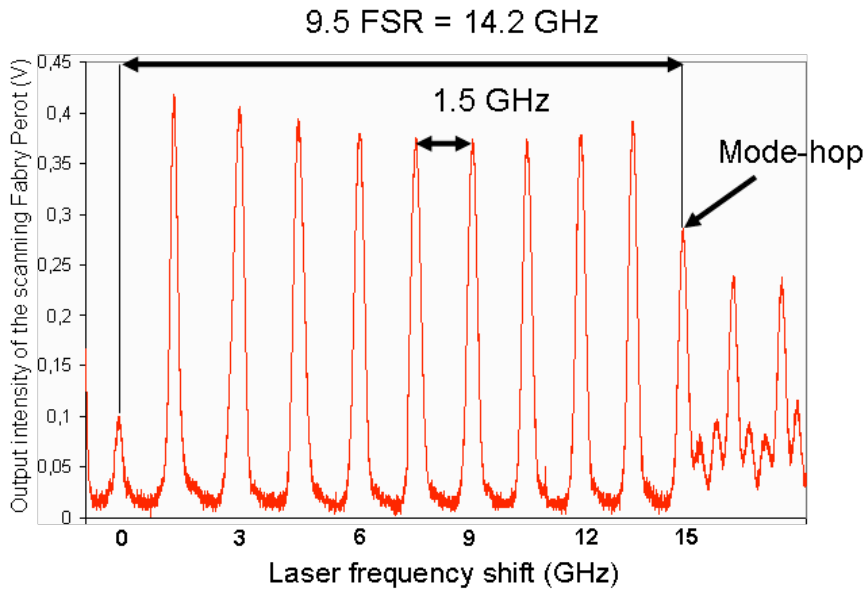


Fig. 9: Continuous tunability of the VECSEL by scanning a 1.5GHz-FSR Fabry Perot

Finally, the laser wavelength has been tuned on the Cesium D2 line. The different transitions from the two hyperfine levels – distant from 9.192 GHz - of the fundamental Cesium atomic level have been scanned on a saturated absorption set-up inside a Cesium cell. A closer look on the transition ( $6^2S_{1/2}, F = 4$ ) towards the excited states ( $6^2P_{3/2}, F'$ ) showed the sub-level transitions. It is worth noticing that we clearly identify on the spectrum in Figure 10 the ( $F = 4 \rightarrow F' = 3/5$ ) and ( $F = 4 \rightarrow F' = 4$ ) transitions that are only distant from 25 MHz, demonstrating a linewidth much narrower than this value. Further characterizations of the VECSEL linewidth are under progress to confirm the suitability of this source for Cs atoms detection; according to published results on optically-pumped VECSEL a linewidth of a few kHz is expected [4,5,11].

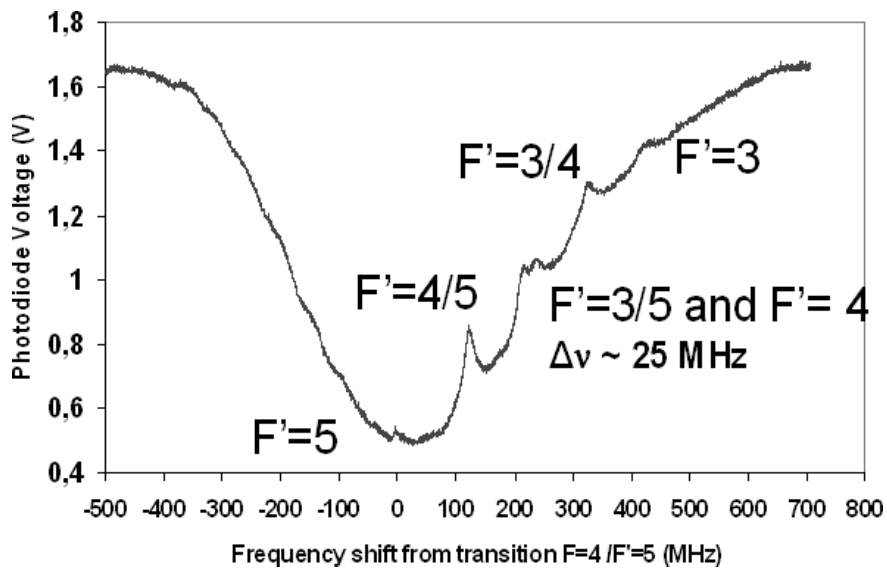


Fig. 10: Scanning of the absorption line from F=4 in a Cesium cell

## CONCLUSION

By giving extra care to the conception and the fabrication of the semiconductor component, we have demonstrated an optically-pumped VECSEL emitting at 852 nm with a low threshold intensity ( $I_{th} = 3 \text{ kW/cm}^2$ ) and an optical gain around 1.5%. We have performed optical and thermal characterizations of this structure in order to optimise its performances. We demonstrated a 330mW laser emission around 852 nm from a structure on a GaAs substrate without any complex additional thermal management. From a diode-pumped single-frequency prototype we have obtained a pump-limited output power of 17 mW on the Cesium  $D_2$  transition. Our source was continuously tunable around the desired wavelength. These results demonstrate the potentialities of our source as an alternative in the optical benches of Cesium atomic clocks. We intend to study further the spectral properties of the laser for the desired metrological applications.

## ACKNOWLEDGEMENTS

This work has been supported by the DGA under the contract Poseida N°0534004. B. Cocquelin acknowledges the CNRS and CNES for the funding of his PhD. The authors acknowledge David Holleville (LNE-SYRTE) for fruitful discussions and for the design of the single-frequency prototype.

## REFERENCES

- 1 Kuznetsov, et al.: "Design and Characteristics of High-Power ( $>0.5 \text{ W CW}$ ) Diode-Pumped Vertical-External-Cavity Surface-Emitting Semiconductor Lasers with Circular  $TEM_{00}$  Beams", IEEE J. of Selected Top. In Quantum Electronics 5, No 3 (1999)
- 2 Lutgen S., Albrecht T., Brick P., Reill W., Luft J. and Späth W. : 8-W high-efficiency continuous-wave semiconductor disk laser at 1000 nm. Applied Physics Letters vol. 82 No 21 (2003)
- 3 J. Chilla, et al.: Proc. SPIE 5332, 143 (2004)
- 4 Garnache A, et al.: "2-2.7 $\mu\text{m}$  single frequency tunable Sb-based lasers operating in CW at RT: Microcavity and External-cavity VCSELs, DFB." Proc. SPIE Semiconductor Lasers and Laser Dynamics Vol. 6184, 61840N (2006)
- 5 Abram R. H., Gardner K. S., Riis E. and Ferguson A. I.: Narrow linewidth operation of a tunable optically pumped semiconductor laser. Optics Express 12, 5434 (2004).
- 6 Lindberg H., Larsson A., and Strassner M.: "Single-frequency operation of a high-power, long-wavelength semiconductor disk laser. Optics Letters vol.30 No17 (2005)
- 7 Coldren L. and Corzine S. : Diode Lasers and Photonic Integrated Circuits. Eds John Wiley & sons (1999)
- 8 Reichling M. and H. Grönbeck: Harmonic heat flow in isotropic layered systems and its use for thin film thermal conductivity measurements. Journal of Applied Physics 75, 1914 (1994).
- 9 Jacquemet, M., Domenech, M., Lucas-Leclin, G., Georges, P., Dion, J., Strassner, M., Sagnes, I., Garnache, A. : Single-Frequency cw vertical external cavity surface emitting semiconductor laser at 1003 nm and 501 nm by intracavity frequency doubling. Applied Physics B 86, 503-510 (2007)
- 10 Hastie, J., et al.: 0.5-W Single Transverse-Mode Operation of an 850-nm Diode-pumped Surface-Emitting Semiconductor Laser. IEEE Photonics Technology Letters, 15, No 7 (2003)
- 11 Holm M., Burns D., Ferguson A. and Dawson M.: Actively stabilized single-frequency vertical-external cavity AlGaAs laser. IEEE Photonics Technology letters vol. 11, No 12 (1999)